Am J Physiol Heart Circ Physiol 286: H113–H120, 2004.
First published September 11, 2003; 10.1152/ajpheart.00587.2003.

Relationship between erythrocyte aggregate size and flow rate in skeletal muscle venules

Jeffrey J. Bishop,[1] Patricia R. Nance,[1] Aleksander S. Popel,[2] Marcos Intaglietta,[1] and Paul C. Johnson[1]
[1]*Department of Bioengineering, University of California, San Diego, La Jolla, California 92093; and*
[2]*Department of Biomedical Engineering, Johns Hopkins University, Baltimore, Maryland 21205*

Submitted 24 June 2003; accepted in final form 3 September 2003

Bishop, Jeffrey J., Patricia R. Nance, Aleksander S. Popel, Marcos Intaglietta, and Paul C. Johnson. Relationship between erythrocyte aggregate size and flow rate in skeletal muscle venules. *Am J Physiol Heart Circ Physiol* 286: H113–H120, 2004. First published September 11, 2003; 10.1152/ajpheart.00587.2003.—In previous studies we showed that intravenous infusion of Dextran 500 in the rat causes blunting of the velocity profile of red blood cells in venules at low shear rates. To determine whether this blunting is associated with the formation of red blood cell aggregates, we measured the length and width of particles in the venular flow stream at systemic hematocrits up to 20% with a high-speed video camera and a new image analysis technique. Data were obtained at various shear rates under normal (nonaggregating) conditions as well as after infusion of Dextran 500. Under normal conditions, particle length (parallel to the vessel axis) was 6.5 ± 2.7 μm and width (perpendicular to the axis) was 6.1 ± 1.7 μm, in agreement with published dimensions of individual red blood cells for this species. After Dextran 500 infusion, particle length and width increased significantly to 8.7 ± 5.1 and 10.4 ± 4.4 μm, respectively. Particle dimensions were greater in the central region of the flow stream for both normal and dextran-treated blood and increased at low flow rates with dextran-treated blood. This study provides direct confirmation of aggregate formation at low shear in venules with high-molecular-weight dextran as well as an estimate of aggregate size and range.

venous vascular resistance; in vivo blood rheology; in vivo microscopy; red blood cell aggregation

PREVIOUS WHOLE ORGAN STUDIES in the cat and dog demonstrated an inverse relationship between blood flow and vascular resistance in the venous network (9, 25, 27, 29, 39). In one of these studies, it was demonstrated that the increase in resistance at low flow rates was nearly abolished in the absence of red blood cell aggregation (9). As a possible mechanism to explain this result, we recently showed (3) that velocity profiles in skeletal muscle venules become significantly blunted compared with Poiseuille flow at low shear rates. This finding is in agreement with previous studies which showed that the velocity profiles of aggregating blood in arterioles, venules, and glass tubes are more blunt than the parabolic shape expected for laminar flow (19, 34, 38). To explain this blunting, we hypothesized the formation of red blood cell aggregates in vivo, with the size of the aggregates inversely related to the shear rate of the blood.

Previous studies showed that the velocity profiles of colloidal suspensions in tube flow become more blunt as the ratio of particle size to tube diameter is increased (7, 8, 34). Studies in rotational viscometers showed that aggregates form at low shear rates (12, 15) and that the size varies inversely with shear rate (35). Although the hypothesis of aggregate formation in venules is consistent with these findings, the difficulty in visualizing red blood cell aggregates with standard video microscopy has precluded verification and quantitative studies in vivo. Video microscopy was used previously to estimate the length of aggregates at low hematocrit (<10%) in a couvette of 40-μm gap width at different shear stresses (1, 11), but to our knowledge there has been no study of aggregate widths (normal to the flow direction) during tube flow either in vitro or in vivo.

To test the hypothesis that aggregates form and that an inverse relationship exists between the size of red blood cell aggregates and the shear rate of blood in vivo, we used a high-speed video camera capable of recording up to 600 frames/s to visualize the flow of red blood cells in venules of the rat spinotrapezius muscle. Studies were performed over a range of physiological flow rates. Red blood cell aggregation was induced by infusion of Dextran 500. To diminish overlapping aggregate images from different vertical planes, systemic hematocrit was reduced to <20%. Because of interference from background structures in the surrounding muscular tissue, it was also necessary, in a number of instances, to utilize an image analysis technique developed specifically for this study. The method determines the light intensity profile along a line segment crossing the venule under study in a direction normal to the blood flow. These intensity profiles were obtained on successive frames and plotted sequentially to recreate images of the red blood cells and aggregates against a background of uniform intensity. Dimensions were determined at various flow rates by using image analysis software with normal (nonaggregating) blood and after administration of Dextran 500.

MATERIALS AND METHODS

Animal preparation. Sixteen male Sprague-Dawley rats weighing between 200 and 350 (278.7 ± 44.6) g were used for these investigations. Animal handling and care were provided following the procedures outlined in the *Guide for the Care and Use of Laboratory Animals* (National Research Council, 1996). The study was approved by the local Animal Subjects Committee. Rats were anesthetized with an intraperitoneal injection of 50 mg/kg pentobarbital sodium (Abbott). Additional anesthetic was administered throughout the experiment as needed. The animal was placed on a heating pad to maintain body temperature during surgery. A trachea tube was inserted to assist breathing, the carotid artery was catheterized for blood withdrawals and pressure measurements, and the jugular vein was catheterized for administration of anesthetic or Dextran 500. All catheters were filled with a solution of heparinized saline (30 IU/ml) to prevent clotting.

Address for reprint requests and other correspondence: P. C. Johnson, Dept. of Bioengineering, Univ. of California, San Diego, La Jolla, CA 92093-0412 (E-mail: pjohnson@bioeng.ucsd.edu).

The costs of publication of this article were defrayed in part by the payment of page charges. The article must therefore be hereby marked "*advertisement*" in accordance with 18 U.S.C. Section 1734 solely to indicate this fact.

The rat spinotrapezius muscle was exteriorized and prepared for intravital microscopy as described previously (2, 3). The animal was then placed on a Plexiglas platform with a raised area that enabled viewing of the muscle while maintaining normal blood flow. The muscle was suffused with Plasma-Lyte A and covered with a thin polyvinyl film (Saran Wrap, Dow Corning) while air bubbles were removed from the muscle surface. A temperature probe was placed beside the muscle so that temperature could be maintained at 37°C throughout the experiment by regulation of a heating element attached to the animal platform.

Microscope system. An intravital microscope (Ortholux II, Leitz) transilluminated with a 100-W mercury arc lamp (model 1149, Walker Instruments, Scottsdale, AZ) was used with Leitz ×25 (numerical aperture 0.6) and Olympus ×40 (0.7) water-immersion objectives and a Leitz UM20 (0.33) condenser lens. A blue filter was used to enhance the contrast between the red blood cells and the background. The image was projected onto a charge-coupled device video camera (MotionCorder Analyzer model 1000, Kodak) capable of recording up to 600 frames/s and storing up to 4,360 frames in internal memory and was viewed on a monitor. This arrangement provided full-screen magnifications of the video image of ×1,620 (160 μm horizontal) and ×2,600 (100 μm horizontal) for the ×25 and ×40 objectives, respectively, on the video monitor (SSM-121, Sony). Recorded frames were transferred to a videocassette recorder (SVO-9500MD, Sony) for storage and later analysis.

Adjustment of red blood cell aggregability and hematocrit. Investigations were performed on animals either under normal (nonaggregating) conditions or after induction of red blood cell aggregation with Dextran 500 (average molecular mass 460 kDa; Sigma) dissolved in saline (6%) and infused in 50 mg/kg increments over the course of 2–3 min (200 mg/kg body wt). This represents a plasma dextran concentration of ~0.6% (3). Although this treatment increases plasma viscosity, such an effect would not affect the present measurements or conclusions. Hematocrit and aggregation index values were determined 15 min after dextran infusion. There was no discernable adverse reaction (e.g., visible swelling of the limbs) to the dextran infusion in any of the rats used for these investigations.

To obtain clear and distinct images of individual red blood cells and aggregates, it was necessary to reduce systemic hematocrit to <20%. Hematocrit reduction was achieved by infusion of autologous plasma obtained by centrifugation of 2–3 ml of whole blood obtained before the experiment was begun. In dextran-treated animals, this procedure was done after infusion of dextran to maintain a concentration of dextran in the plasma similar to that in our previous studies (2–6). Mean arterial pressure was monitored during and after blood withdrawal and plasma infusion until a steady-state value was reestablished that was not significantly different from the control value.

Hematocrit, aggregation, and pressure measurements. The hematocrit and degree of red blood cell aggregation were measured during the control period as well as after infusion of Dextran 500. Hematocrit was determined after centrifugation with a microhematocrit centrifuge (Readacrit, Clay Adams). The degree of red blood cell aggregation (M) was assessed from triplicate measurements on a 0.35-ml blood sample with a photometric rheoscope (Myrenne Aggregometer, Myrenne, Roetgen, Germany) on the 10-s setting. The carotid artery catheter was attached to a pressure transducer (TNF-R, Viggo Spectramed) connected to a strip chart recorder (Brush 2600, Gould) for determination of arterial pressure. Pressure was recorded continuously throughout the experimental protocol and manually transferred into a microcomputer (550-MHz Pentium III, Dell) from the strip chart recordings for later analysis.

Experimental protocol. Venules of 53 ± 17-μm diameter (range 27–107 μm) with no side branches in the field of view were selected for study on the basis of the criteria of stable flow as well as clear focus and contrast of the image. The microscope was focused on the equatorial plane of the venule, and the video camera was oriented with the venule longitudinal axis horizontally on the video screen. In some instances, it was necessary to either elevate or reduce the arterial pressure to obtain pseudoshear rates (mean velocity/diameter) distributed throughout the desired experimental range (1–85 s^{-1}). Elevation of arterial pressure was accomplished by the gradual infusion of 1 ml of 6% epinephrine (Sigma) over ~10 s. Reduction of arterial pressure was accomplished by blood withdrawal via the carotid artery into a heparinized syringe. In a previous investigation, we reported (2) that the diameter reduction that occurred in these vessels during this protocol of blood withdrawal was very minor, ~2%, regardless of venular orientation. After stabilization of blood flow, the framing rate and shutter open duration were adjusted to maximize image clarity for the specific flow and background conditions. A video image of the vessel was recorded into the memory of the high-speed camera, after which it was played back and recorded onto a standard SVHS videotape at 30 frames/s. If blood was withdrawn it was reinfused, and in all cases the arterial pressure was monitored until it returned to a steady-state value that was not significantly different from control. At this point, another suitable venule was selected and the experimental protocol was repeated.

Image analysis. Measurements of red blood cell or aggregate size were made by analysis of digitized video frames of the recorded flow with an image analysis software package (SigmaScan Pro 5.0, SPSS). For this purpose, the videocassette recorder was connected to a video capture board (DC30 plus, miroVIDEO) installed in a microcomputer (300-MHz Pentium II, Micron) and the video frames were digitized with Adobe Premier 4.0 (Adobe), after which the image files were transferred to a compact disk (CD-Writer Plus 7200e, Hewlett-Packard) for analysis and storage. Image magnification was determined from the recorded image of a stage micrometer under transillumination.

Measurements of either length (parallel to the flow direction) or width (normal to the flow direction) were only made on particle images that had distinct edges. Particles that had irregular (i.e., T- or L shaped) shapes were assumed to be multiple separate particles in different vertical planes whose images were overlapping and as such were not measured. A wide variety of shapes, including cylindrical, spherical, and other shapes with regular borders, were routinely observed and measured. Whenever possible, the movement of particles was observed during slow-motion playback of the videotape to confirm that they consisted of one aggregate moving as a uniform body and not as multiple aggregates moving and rotating separately.

In some instances, the recorded images were sufficiently clear to obtain measurements of red blood cell or aggregate size directly from the digitized video frames. However, as shown in the sample video micrograph of dextran-treated blood (Fig. 1*A*), background structures in the surrounding tissue were frequently present and obscured the exact location of the peripheral border of red blood cells and aggregates. To circumvent this problem, the intensity of a single line of pixels across the venule lumen was monitored with the image analysis software package. A short length of the venule with uniform background was selected, and line intensity scans from ~200 sequential video frames were plotted to recreate an image of those cells and aggregates that crossed the reading line. A sample image created from the line intensity scans performed on this venule is shown in Fig. 1*B*. Calibration of radial distance was accomplished from the recorded image of a stage micrometer. For longitudinal distance, calibration was determined from the framing rate of the video camera and by velocity determinations made at each radial position by the dual-slit technique of Wayland and Johnson (41) modified for analysis of video images as described by Intaglietta et al. (26). Images like that shown in Fig. 1*B* were drawn for each vessel based on the center line velocity, and measurements of length taken at other radial positions were then scaled based on the velocity at that radial position. The method was validated by comparing cell and aggregate size with this method to measurements made directly off the videotape images in instances where interference from background structures was minimal (see RESULTS).

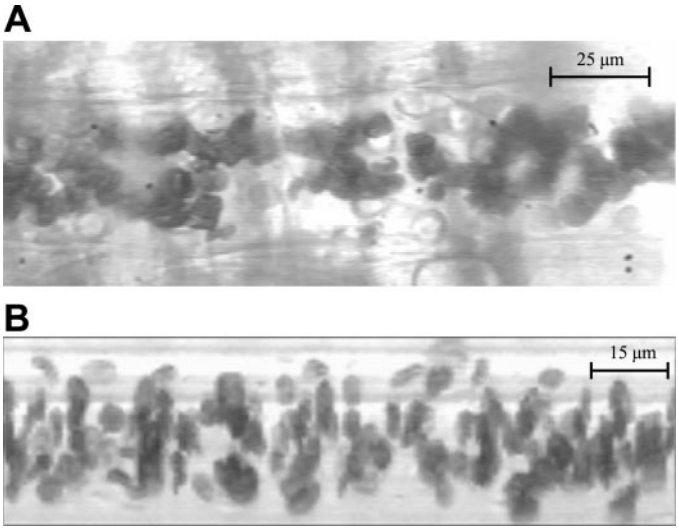

Fig. 1. *A*: sample videomicrograph of a 38-μm venule with dextran-treated, aggregating blood flowing through it at a hematocrit of 19%. The picture is a still frame recording at 120 frames/s of blood flowing at a pseudoshear rate of 7 s^{-1}. Note the interference of background structures from the surrounding muscle that frequently obscure the dimensions of red blood cells and aggregates. *B*: image of vessel in *A* after processing with the line intensity scan method and calibration for center line velocity. Note the homogeneous background against which the dimensions of red blood cells and aggregates may be determined.

Statistical analysis. Both the *t*-test and the nonparametric Mann-Whitney's rank sum test were used to determine differences in experimental and physiological parameters between normal and dextran-treated animals. Values for mean arterial pressure, aggregation index M, and hematocrit are reported as means ± SD. Correlation coefficients and probability values were calculated with a standard software package (Excel, Microsoft). Differences in parameters between normal and dextran-treated rats were determined with both the paired *t*-test and the nonparametric Wilcoxon signed-rank test performed by a statistical software package (SigmaStat, Jandel). For all tests and regression fits, $P < 0.05$ was considered statistically significant.

RESULTS

Hematocrit, degree of aggregation, and arterial pressure. Under control conditions for normal rats, the hematocrit was 42.7 ± 4.8%, the index of aggregation M was 0.0 in all cases, and the mean arterial pressure was 108 ± 15 mmHg. After administration of Dextran 500, the hematocrit was 43.6 ± 4.5%, M was 10.7 ± 5.6, and the mean arterial pressure was 109 ± 16 mmHg. There were no significant differences ($P > 0.05$) between either the hematocrit or the mean arterial pressure of normal and dextran-treated animals during the control situation. After hematocrit reduction as described in *Adjustment of red blood cell aggregability and hematocrit*, systemic hematocrit was reduced to 15.1 ± 2.7% (range 9.8–19.0%). Reduction of flow rate was obtained by blood withdrawal into a heparinized syringe as explained in *Experimental protocol*. Pseudoshear rate values in the range of 1–85 s^{-1} were obtained at mean arterial pressures of 18–100 mmHg.

Validation of image processing method. To validate the line intensity scan method for determining dimensions of cells and aggregates in the flow stream described in MATERIALS AND METHODS, we videotaped several venular sites where measurement of particles (cells or aggregates) directly from the video image was also possible. We compared the dimensions of >250 particles measured under both normal and dextran-treated conditions manually from the image recorded on videotape and also with the image analysis method described in *Image analysis*.

For one vessel under normal conditions (diameter = 50 μm, Hct = 16%, pseudoshear rate = 3 s^{-1}), the average particle width as measured by the image processing method was 6.2 ± 1.5 μm (range 3.7–8.9 μm), not significantly ($P = 0.56$) different from the average of 6.0 ± 1.9 μm (range 2.3–10.0 μm) obtained by direct measurement of the recorded video image without processing. Average particle length obtained by the image processing method was 6.4 ± 1.8 μm (range 3.1–8.7 μm), not significantly ($P = 0.88$) different from the average of 6.5 ± 2.6 μm (range 2.5–15.5 μm) obtained by direct measurement. For one vessel under dextran-treated conditions (diameter = 38 μm, Hct = 19%, pseudoshear rate = 7 s^{-1}), the average particle width as measured by the image processing method was 7.6 ± 3.6 μm (range 3.1–18.2 μm), not significantly ($P = 0.11$) different from the average of 7.0 ± 2.9 μm (range 2.6–17.0 μm) obtained by direct measurement. Average particle length obtained by the image processing method was 8.2 ± 5.8 μm (range 2.1–24.4 μm), not significantly ($P = 0.34$) different from the average of 7.7 ± 3.5 μm (range 2.5–25.0 μm) obtained by direct measurement.

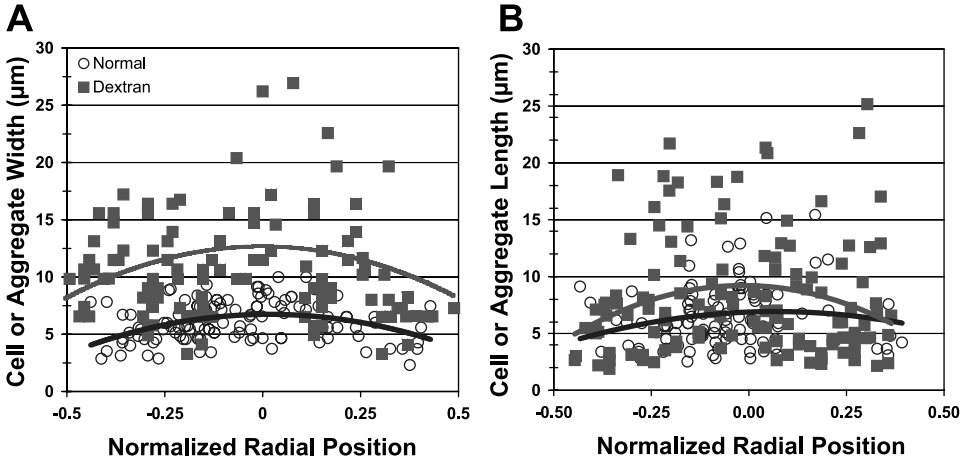

Fig. 2. Red blood cell or aggregate width (*A*) and length (*B*) vs. normalized radial position for normal (vessel diameter = 50 μm, Hct = 16%, pseudoshear rate = 3 s^{-1}; $n = 155$) and dextran-treated (vessel diameter = 38 μm, Hct = 19%, pseudoshear rate = 7 s^{-1}; $n = 116$) blood. Lines represent second-order polynomial fits to the individual data points. Note that aggregate size corresponds to the size of individual red blood cells (diameter = 6.8 μm) in the absence of dextran and in the high-shear region near the wall when aggregation is present but increases in the low-shear central region of the venule when dextran is present.

Length and width of red blood cells and aggregates. With the image processing method, length and width measurements were made in 45 venules (53 ± 17-μm diameter, range 27–107 μm) to obtain measurements of over 1,250 cells and/or aggregates. For the entire population of cells studied, the measured particle length under normal conditions was 6.5 ± 2.7 μm and the measured width was 6.1 ± 1.7 μm. After dextran infusion, the measured length of red blood cells or aggregates was 8.7 ± 5.1 μm and the measured width was 10.4 ± 4.4 μm. Measurements of both lengths and widths under normal conditions were significantly different ($P < 0.01$) from the corresponding values after dextran infusion. A substantial dispersion among individual values is not unexpected. The shape of the velocity profile and hence the radial shear rate gradient vary from vessel to vessel with aggregability and flow rate, so red blood cells located at different radial positions or in different vessels may experience widely different local shear rate environments. Data for a single venule are shown in Fig. 2, in which the width (Fig. 2*A*) and length (Fig. 2*B*) of a number of red blood cells and aggregates under normal conditions and after dextran infusion are presented as a function of radial position.

For normal blood, both the width and length of individual particles at this pseudoshear rate (3 s^{-1}) are a function of radial position. This relationship is more evident in width, with the mean value of the trend line falling to 4 μm near the wall and rising to ~6.5 μm at the center. The width of the cells is, on the average, less than the unstressed diameter of the rat red blood cell, 6.8 μm. Length values for normal blood show similar trends of mean values with radial position, but the effect of radial position is somewhat less. In addition, length values are more disperse than those for width and reach higher values as described in more detail in Fig. 3. The overall mean value for length is also somewhat less than the unstressed diameter of the rat red blood cell.

In dextran-treated blood, at a pseudoshear rate of 7 s^{-1}, it is apparent that both mean width and length of individual particles show a dependence on radial position as seen with normal blood, whereas individual values show a considerably greater dispersion. The mean particle width after dextran treatment is consistently ~6 μm greater than that of the normal blood. Mean particle length after dextran infusion is virtually identical to normal blood at the vessel wall but is ~2 μm greater in the center of the vessel. The range of individual values in the center of the flow stream is described in more detail in Fig. 3.

The values of particle length and width from the population of cells studied ($n = 1,250$) are plotted as histograms in Fig. 3*A* for normal blood and in Fig. 3*B* for dextran-treated blood. From Fig. 3*A* it can be seen that the distribution of length and width values for normal blood is similar except that 10% of the values for length fall beyond the maximum value for width (10 μm) and reach 16 μm. The minimum values are ~3 μm in both cases.

As shown in Fig. 3*B*, the distribution of length and width of particles after dextran treatment is somewhat different. Although the range is similar for both dimensions, 36% of length values are below 7 μm whereas only 8% of width values fall in this range. The difference may reflect the orientation of individual red blood cells as shown in Fig. 1*B*, where it appears that many of the cells in the center of the flow field are oriented normal to the flow stream. The maximum values for length and width in dextran-treated blood are ~25 μm, which is well beyond that for normal blood.

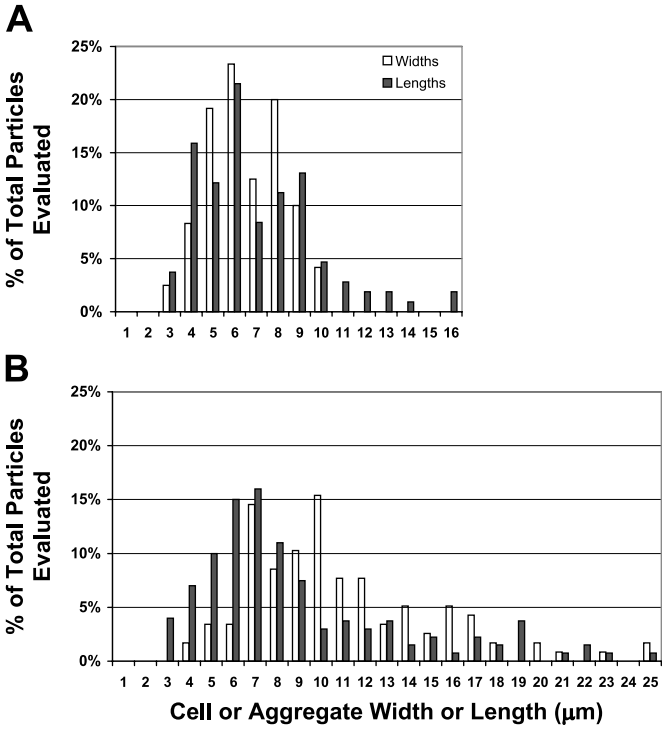

Fig. 3. Histogram plots of the entire population ($n = 1,250$) data for red blood cell or aggregate width and length for normal (*A*) and dextran-treated (*B*) blood. For normal blood, a slight tendency for aggregation in the longitudinal direction is suggested by the several lengths measured to be >10 μm whereas cell widths are evenly distributed about the value of the red blood cell diameter (6.8 μm). Distributions for both length and width are similar for dextran-treated blood. Under these conditions, aggregates form and grow to several times the size of individual red blood cells.

In comparing normal and dextran-treated blood several differences are apparent. The maximum values for the latter are ~50% greater than for the former. Forty-four percent of the width values are beyond the maximum width for normal blood (10 μm), but only twelve percent of length values after dextran treatment exceed the length values seen with normal blood. However, 29% of the length values after dextran treatment exceed 10 μm whereas in normal blood only 10% of length values do.

Relationship between pseudoshear rate and particle size. In this study the average width of at least 30 red blood cells or aggregates at the center line of each of the vessels studied was determined, and the pooled results are shown in Fig. 4 vs. the pseudoshear rate in the venule. Over the shear rate range shown, the width of individual particles in normal blood is independent of shear rate and is close to the size of an individual rat red blood cell (6.8 μm). At the highest shear rates, the majority of values are less than this dimension. At the lowest shear rates, there appears to be a slight but nonsignificant increase in particle size above the diameter of a single red blood cell.

The width of individual particles in dextran-treated blood is significantly ($P < 0.001$) larger than in normal blood at the lowest pseudoshear rates. Although a polynomial regression was used to fit the dextran-treated data in Fig. 4, it is possible

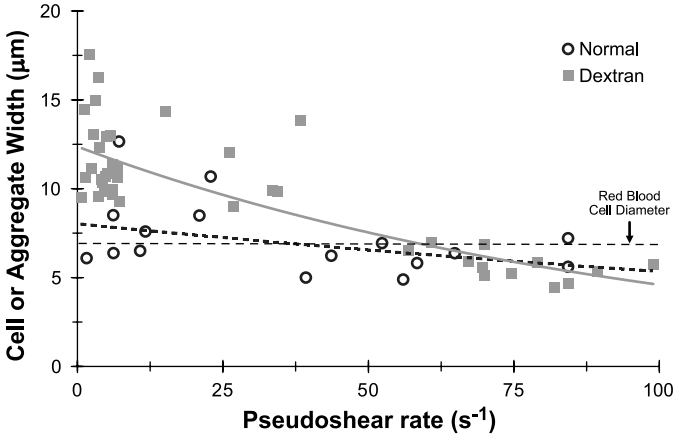

Fig. 4. Pooled results showing the average red blood cell or aggregate width at vessel center line vs. the vessel pseudoshear rate for normal (n = 16 vessels) and dextran-treated (n = 42 vessels) blood. Average particle width is not significantly different from the diameter of a single red blood cell under normal conditions at all investigated shear rates, whereas for dextran-treated blood average particle size rises to nearly twice the size of a single red blood cell at the lowest shear rates. The regression lines shown are linear (bold dotted line; r^2 = 0.2) and second-order polynomial (solid gray line; r^2 = 0.76) fits for normal and dextran-treated points, respectively.

that a different function might describe the relationship equally well. Specifically, it appears that a step function might be appropriate because, on average, aggregates are two to three times wider than the diameter of a single red blood cell at pseudoshear rates less than ~40 s^{-1}, whereas at pseudoshear rates >50 s^{-1} the average width of individual particles approaches the red blood cell diameter and is not significantly different from the value obtained with normal blood at similar pseudoshear rates. It is of interest that at these highest pseudoshear rates the particle size for dextran-treated blood consistently falls below the unstressed diameter of the red blood cell, indicating that the blood is effectively disaggregated and red blood cells may be oriented in the direction of the flow stream.

Shape and orientation of aggregates in a flow stream. Paired measurements of length and width for ~300 cells and aggregates are shown in Fig. 5. On an individual basis the values for length and width appear to be related for both normal and dextran-treated blood. The slope is not significantly different for the two conditions, with length being somewhat greater than width.

DISCUSSION

Formation of red blood cell aggregates. The purpose of this study was to verify the formation of red blood cell aggregates in venules in the presence of Dextran 500 and to obtain quantitative information on aggregate size in relation to shear rate. It has long been known that in the presence of long-chain macromolecules red blood cells tend to form clusters or aggregates. It is estimated that the forces involved are <1 dyn/cm^2 (14) and thus are found only in flow regimes of low shear stress.

Current information on the formation of aggregates and the relation between aggregate size and shear rate is based almost entirely on in vitro and theoretical studies (1, 10, 13, 17, 20–22, 30, 32, 33, 35, 40). Using a transparent cone-plate viscometer, Schmid-Schönbein et al. (35) reported that visible aggregates formed in human blood at shear rates below 46 s^{-1} and were nearly uniform in size at any given shear rate. The characteristic length was inversely related to the shear rate and increased to >15 μm at the lowest shear rates (~5 s^{-1}). Also using human blood, Goldsmith and coworkers (20–22) reported that linear (rouleaux) and branched aggregates of up to 20 erythrocytes could be seen at shear rates of <4 s^{-1} but that only single cells were observed at shear rates >50 s^{-1}. Similar studies by Shiga et al. (36, 37) showed that typical aggregates contained 10–20 erythrocytes at low (7.5 s^{-1}) shear rates. More recently, Yedgar and coworkers (1, 11) used a cell flow properties analyzer (40-μm-wide channel) to measure human red blood cell aggregate dimensions at 10% hematocrit. They found small aggregates (3 to 4 red blood cells) beginning at shear rates below ~67 s^{-1}, which increased in size up to 17–32 red blood cells/aggregate with decreasing shear rate to <5 s^{-1}.

In our study aggregates were more common in the center of the flow stream than near the vessel wall, although aggregates were not absent from the wall region, as shown in Fig. 2. The presence of aggregates near the wall is probably due to the branching nature of the venular network and infusion of aggregates from tributary vessels into the flow stream as we

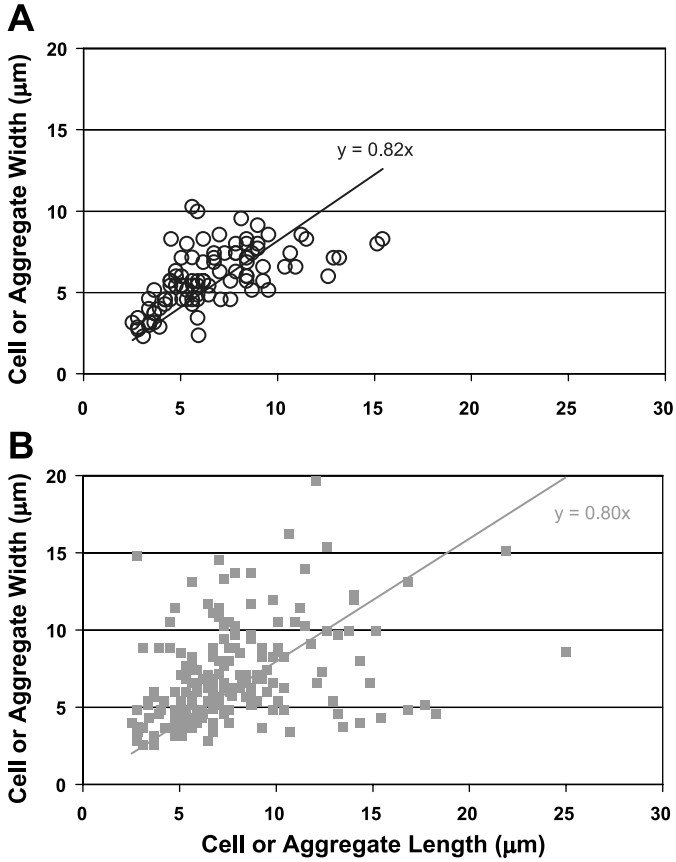

Fig. 5. Paired measurements (n = 291) of the length and width of individual red blood cells and aggregates in normal (*A*) and dextran-treated (*B*) rats to show the manner in which red blood cell aggregates enlarge in the flow stream. The slopes of the regression lines for normal (y = 0.82x) and dextran-treated (y = 0.80x) conditions are not significantly different from one another, indicating that in venules of the size (27–107 μm) and shear rate (1–100 s^{-1}) studied here single red blood cells are preferentially oriented so as to be aligned with the flow and aggregates are slightly longer (longitudinal dimension) than they are wide (radial dimension).

suggested previously (9). In this venule the center line velocity is 266 μm/s, and the distance between the branch points in 50 μm venules in this muscle is ~190 μm (5). In support of this suggestion, we found previously (5) that labeled red blood cells entering from a tributary tended to remain near the wall of the vessel during travel downstream.

We found a wide distribution of particle dimensions in the center of the flow stream from 3 μm, characteristic of a red blood cell viewed edge-on, to dimensions of red blood cell aggregates in low shear flow up to 25 μm. The presence of aggregates in this region is expected because the shear rate is lower in the central region of the vessel than it is near the vessel wall and is therefore conducive to aggregate formation. The presence of individual cells in this region of low shear was also expected because of infusion of cells and aggregates from tributaries and the reduction of systemic hematocrit. It should be noted that we are only able to make two-dimensional measurements of a three-dimensional flow system. We cannot exclude the possibility that some of the particles we attribute to the horizontal plane at the center of the flow stream were above this plane in the high-shear-rate region near the vessel wall.

If we assume that the aggregates we studied are symmetrical in the radial dimension, a calculation of the volume they would occupy divided by the known volume of a single red blood cell shows that the largest aggregates at the lowest shear rates (1–5 s^{-1}) would contain between 10 and 25 red blood cells. Although this is the first study known to the authors in which a direct measurement of aggregate size was done in vivo, the close agreement to the range found in previous in vitro studies suggests that the relationship between the size of red blood cell aggregates and the local shear rate is similar for both systems.

It is of interest that in both normal and dextran-treated blood, the particle dimension in the direction of flow was somewhat greater than in the radial direction as shown in Fig. 5. With normal blood this difference may indicate a process of minimizing the cross-sectional area of individual red blood cells in the radial direction where the shear stress is greatest. A similar preferential orientation of aggregates would also be expected. However, we often observed aggregate tumbling in our studies that would limit the asymmetry of an aggregate.

The only previous report of aggregate size in vivo was that of Osterloh et al. (31), who used a Fourier analysis of recorded light intensity patterns to determine the characteristic particle length in rat mesenteric arterioles and venules 20–35 μm in diameter. Their analysis obtained a pattern size in normal blood of 11.4 ± 3.1 μm at a pseudoshear rate of 200 s^{-1}, which rose to 16.7 ± 6.0 μm at 75 s^{-1}. After dextran 250 infusion the pattern size was 15.3 ± 4.5 μm at 227 s^{-1} and rose to 20.8 ± 5.5 μm at 28 s^{-1}. The authors noted that pattern size would reflect dimensions of plasma gaps and white blood cells as well as red blood cells and aggregates. Although direct comparison with our findings is limited because their studies were generally carried out at higher shear rates and at nonreduced hematocrits, their particle length was about twice our values at similar shear rates. We did see similar trends for an increase in particle width for normal and dextran-treated blood as they saw for length when shear rate was lowered. However, their pattern size also increased when shear rate was increased to 600–1,000 s^{-1}. The authors suggested that nonaggregating cells may form short-lived clusters brought together by hemodynamic forces.

Ultrasound backscattered power has also been used to characterize erythrocyte aggregation in vivo, although the method is limited to large vessels (16). The integrated backscatter power of aggregating blood is linearly proportional to the number of red blood cells per aggregate and is shear rate dependent between 1 and 100 s^{-1}. As shown in Fig. 4, our studies suggest aggregate size dependence on shear rate in the same shear rate range.

Effect of hematocrit on aggregate size. Ultrasound studies report a maximum aggregate size at hematocrits of 25–30%, in agreement with theoretical studies (23). The normal hematocrit in the venules we studied would be in this same range (26–30%), based on studies in cat sartorius muscle (24) and cat mesentery (29). With systemic hemodilution, venular hematocrit falls in proportion to systemic hematocrit according to studies in cat mesentery (28). Thus in our study venular hematocrit would fall to ~35% of its normal value, or 10%. Given the relationship between hematocrit and aggregate size shown in ultrasound studies, aggregate dimensions under dextran-treated conditions and at normal hematocrits would be slightly larger than those presented here.

Relationship of red blood cell alignment, deformability, and aggregation with shear rate. As discussed above, the size of red blood cell aggregates increases to several times the size of an individual red blood cell in low-shear-rate regions. Also illustrated in Fig. 4 is the observation that at high shear rate, the width of red blood cells is, on the average, less than the unstressed diameter of a rat red blood cell (major axis 6.8 μm). For a human red blood cell at rest the minor axis width is approximately one-fourth the diameter of the major axis (18). By integration of the two-dimensional shape projected by a red blood cell randomly rotating in three dimensions, we estimate

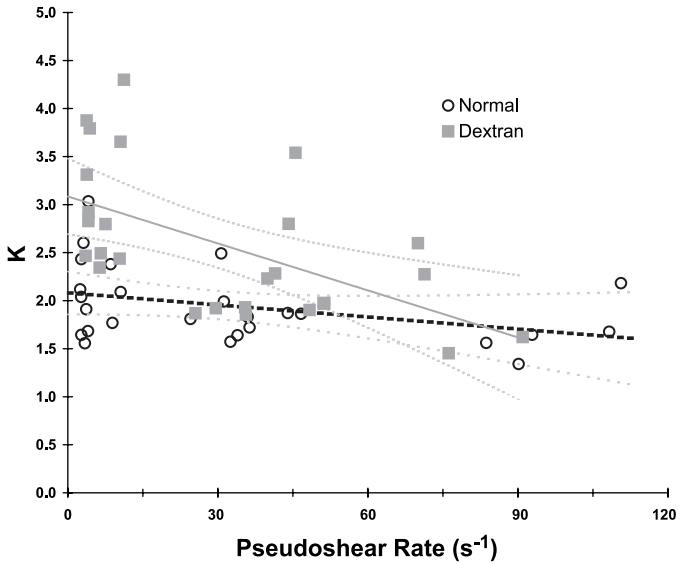

Fig. 6. Velocity profile bluntness parameter K vs. pseudoshear rate for normal and dextran-treated rats (adapted from Fig. 10 in Ref. 3). As explained in detail in Ref. 3, K is the exponent in the parabolic equation used to describe the shape of the velocity profile. $K = 2$ for a parabolic flow profile, and $K > 2$ for profiles that are more blunt than a parabolic shape. Note that with dextran-treated blood, velocity profiles in venules of the size studied here begin to blunt at pseudoshear rates <40 s^{-1}. The dotted lines represent 95% confidence intervals. A similar relationship between pseudoshear rate and aggregate width was shown in Fig. 4 of the present study.

that the average width of a red blood cell image would be ~6.1 μm for rat red blood cells. This is identical to our mean value of width obtained at the center of the flow stream of 6.11 ± 1.75 μm. The mean length was slightly greater (6.49 ± 2.71 μm). As shown in Fig. 5, the measured width of red blood cells at shear rates >75 s^{-1} is less than this value. This observation is consistent with previous in vitro observations showing that red blood cells align with the direction of flow and then deform to even smaller widths at high shear rates (20).

Relationship between aggregate size and shape of velocity profiles. It was shown previously that velocity profiles of human blood become more blunted (compared with parabolic Poiseuille flow) when the particle size-to-tube diameter ratio is increased (7, 8, 34). In this regard, it is evident that the width of aggregates is a much more important determinant of velocity profile than the length of aggregates because the latter are parallel to the flow stream. In our study particle width varies widely. For example, in Fig. 2*A* we note that after dextran treatment mean particle width varies from 8 μm to 12 μm in this 38-μm vessel and at most radial positions a significant number of aggregates >15 μm wide may be found. (Note that the graph symbols depict location of the aggregate center but not its width.) In general we found that individual aggregates in venules of 27–107 μm are two to four times wider than the diameter of individual red blood cells at pseudoshear rates less than ~40 s^{-1}. The dependence of aggregate width on shear rate is consistent with our earlier finding (3) that the degree of blunting of velocity profiles of dextran-treated blood in these vessels is dependent on pseudoshear rate in the same range of shear rates. Figure 4 can be compared with Figure 6, adapted from Ref. 3, in which a velocity profile bluntness parameter (*K*) value of 2.0 represents a parabolic velocity profile and higher values represent increased blunting of the profile. It was shown in that study (3) that the increased blunting of the velocity profiles that is seen over the same arterial pressure and shear rate ranges studied here could explain an increase in venous vascular resistance of ~100% if the hematocrit near the venular wall did not decrease significantly on flow reduction due to an increase in the rate of axial migration of red blood cell aggregates. In recent studies, we have shown (4–6) that the flow rate and branching pattern of the venular network do not allow for significant axial migration of red blood cells or aggregates over this shear rate range and that random cellular dispersions are similar in magnitude to the rate of axial migration of individual particles. These findings, together with the present study, strongly support previous suggestions (34) based on indirect evidence that the blunted velocity profile in tube flow with increased red blood cell aggregability is due to the formation of aggregates. Moreover, it appears that aggregate size in the central region of venules of 27- to 107-μm diameter is not dissimilar from those seen in in vitro studies at similar shear rates. The present findings, together with our recent studies (2–6), also provide additional support for the conclusion of an earlier study that the formation of red blood cell aggregates is largely responsible for the inverse relationship between flow rate and venous vascular resistance (9).

ACKNOWLEDGMENTS

The authors thank Masoud Paknejad and Rami Apelian for technical assistance in data acquisition.

GRANTS

This work was supported by National Heart, Lung, and Blood Institute Grants HL-52684, HL-64395, and HL-62354.

REFERENCES

1. **Barshtein G, Wajnblum D, and Yedgar S.** Kinetics of linear rouleaux formation studied by visual monitoring of red cell dynamic organization. *Biophys J* 78: 2470–2474, 2000.
2. **Bishop JJ, Nance P, Popel AS, Intaglietta M, and Johnson PC.** Diameter changes in skeletal muscle venules during arterial pressure reduction. *Am J Physiol Heart Circ Physiol* 279: H47–H57, 2000.
3. **Bishop JJ, Nance P, Popel AS, Intaglietta M, and Johnson PC.** Effect of erythrocyte aggregation on velocity profiles in venules. *Am J Physiol Heart Circ Physiol* 280: H222–H236, 2001.
4. **Bishop JJ, Nance P, Popel AS, Intaglietta M, and Johnson PC.** Erythrocyte margination and sedimentation in skeletal muscle venules. *Am J Physiol Heart Circ Physiol* 281: H951–H958, 2001.
5. **Bishop JJ, Popel AS, Intaglietta M, and Johnson PC.** Effects of erythrocyte aggregation and venous network geometry on red cell axial migration. *Am J Physiol Heart Circ Physiol* 281: H939–H950, 2001.
6. **Bishop JJ, Popel AS, Intaglietta M, and Johnson PC.** Effect of shear rate and aggregation on the dispersion of red blood cells flowing in venules. *Am J Physiol Heart Circ Physiol* 283: H1985–H1996, 2002.
7. **Brooks DE, Goodwin JW, and Seaman GVF.** Interactions among erythrocytes under shear. *J Appl Physiol* 28: 172–177, 1970.
8. **Bugliarello G and Hayden JW.** Detailed characteristics of the flow of blood in vitro. *Trans Soc Rheol* 7: 209–230, 1963.
9. **Cabel M, Meiselman HJ, Popel AS, and Johnson PC.** Contribution of red blood cell aggregation to venous vascular resistance in skeletal muscle. *Am J Physiol Heart Circ Physiol* 272: H1020–H1032, 1997.
10. **Chen J and Huang Z.** Analytical model for effects of shear rate on rouleau size and blood viscosity. *Biophys Chem* 58: 273–297, 1996.
11. **Chen S, Gavish B, Zhang S, Mahler Y, and Yedgar S.** Monitoring of erythrocyte aggregate morphology under flow by computerized image analysis. *Biorheology* 32: 487–496, 1995.
12. **Chien S.** Shear dependence of effective cell volume as a determinant of blood viscosity. *Science* 168: 977–978, 1970.
13. **Chien S and Sung LA.** Physicochemical basis and clinical implications of red cell aggregation. *Clin Hemorheol* 7: 71–91, 1987.
14. **Chien S, Sung LA, Kim S, Burke AM, and Usami S.** Determination of aggregation force in rouleaux by fluid mechanical technique. *Microvasc Res* 13: 327–333, 1977.
15. **Chien S, Usami S, Dellenback RJ, and Gregersen MI.** Shear-dependent interaction of plasma proteins with erythrocytes in blood rheology. *Am J Physiol* 219: 143–153, 1970.
16. **Cloutier G and Qin Z.** Ultrasound backscattering from non-aggregating and aggregating erythrocytes: a review. *Biorheology* 34: 443–470, 1997.
17. **Dintenfass L, Jedrzejczyk H, and Willard A.** Application of stereological methods to evaluation of aggregation of red cells in 12.5 μm slit: a photographic and statistical study. *Biorheology* 18: 387–404, 1981.
18. **Fung YC.** *Biomechanics: Mechanical Properties of Living Tissue*. New York: Springer, 1993.
19. **Gaehtgens P, Meiselman HJ, and Wayland H.** Velocity profiles of human blood at normal and reduced hematocrit in glass tubes up to 130 μ diameter. *Microvasc Res* 2: 13–23, 1970.
20. **Goldsmith HL.** Microscopic flow properties of red cells. *Fed Proc* 26: 1813–1820, 1967.
21. **Goldsmith HL and Marlow J.** Flow behaviour of erythrocytes. I. Rotation and deformation in dilute suspensions. *Proc R Soc Lond B Biol Sci* 182: 351–384, 1972.
22. **Goldsmith HL and Mason SG.** The flow of suspensions through tubes. I. Single spheres, rods, and disks. *J Colloid Sci* 17: 448–476, 1962.
23. **Hanss M and Boynard M.** Ultrasound backscattering from blood: hematocrit and erythrocyte aggregation dependence. In: *Ultrasonic Tissue Characterization II*, edited by Linzer M. Gaithersburg, MD: National Bureau of Standards, 1979, p. 165–169.
24. **House SD and Johnson PC.** Diameter and blood flow of skeletal muscle venules during local flow regulation. *Am J Physiol Heart Circ Physiol* 250: H828–H837, 1986.
25. **House SD and Johnson PC.** Microvascular pressure in venules of skeletal muscle during arterial pressure reduction. *Am J Physiol Heart Circ Physiol* 250: H838–H845, 1986.

26. **Intaglietta M, Thompkins WR, and Richardson DR.** Velocity measurements in the microvasculature of the cat omentum by on-line method. *Microvasc Res* 2: 151–162, 1970.
27. **Johnson PC and Hanson KM.** Effect of arterial pressure on arterial and venous resistance of intestine. *J Appl Physiol* 17: 503–508, 1962.
28. **Lipowsky HH and Firrell JC.** Microvascular hemodynamics during systemic hemodilution and hemoconcentration. *Am J Physiol Heart Circ Physiol* 250: H908–H922, 1986.
29. **Lipowsky HH, Usami S, and Chien S.** In vivo measurements of "apparent viscosity" and microvessel hematocrit in the mesentery of the cat. *Microvasc Res* 19: 297–319, 1980.
30. **Muralidharan E.** Simultaneous determination of hematocrit, aggregate size, and sedimentation velocity by He-Ne laser scattering. *Biorheology* 31: 587–599, 1994.
31. **Osterloh K, Gaehtgens P, and Pries AR.** Determination of microvascular flow pattern formation in vivo. *Am J Physiol Heart Circ Physiol* 278: H1142–H1152, 2000.
32. **Perelson AS and Weigel FW.** The equilibrium size distribution of rouleaux. *Biophys J* 37: 515–522, 1982.
33. **Pribush A, Meiselman HJ, Meyerstein D, and Meyerstein N.** Dielectric approach to investigation of erythrocyte aggregation. II. Kinetics of erythrocyte aggregation-disaggregation in quiescent and flowing blood. *Biorheology* 37: 429–441, 2000.
34. **Schmid-Schönbein GW and Zweifach BW.** RBC velocity profiles in arterioles and venules of the rabbit omentum. *Microvasc Res* 10: 153–164, 1975.
35. **Schmid-Schönbein H, Gaehtgens P, and Hirsch H.** On the shear rate dependence of red cell aggregation in vitro. *J Clin Invest* 47: 1447–1454, 1968.
36. **Shiga T, Imaizumi K, Harada N, and Sekiya M.** Kinetics of rouleaux formation using TV image analyzer. I. Human erythrocytes. *Am J Physiol Heart Circ Physiol* 245: H252–H258, 1983.
37. **Shiga T, Imaizumi K, Maeda N, and Kon K.** Kinetics of rouleaux formation using TV image analyzer. II. Rat erythrocytes. *Am J Physiol Heart Circ Physiol* 245: H259–H264, 1983.
38. **Tangelder GJ, Slaaf DW, Muijtjens AMM, Arts T, oude Egbrink MGA, and Reneman RS.** Velocity profiles of blood platelets and red blood cells flowing in arterioles of the rabbit mesentery. *Circ Res* 59: 505–514, 1986.
39. **Thulesius O and Johnson PC.** Pre- and postcapillary resistance in skeletal muscle. *Am J Physiol* 210: 869–872, 1966.
40. **Usami S, King RG, Chien S, Skalak R, Huang CR, and Copley AL.** Microcinephotographic studies on red cell aggregation in steady and oscillatory shear—a note. *Biorheology* 12: 323–325, 1975.
41. **Wayland H and Johnson PC.** Erythrocyte velocity measurement in microvessels by a two-slit photometric method. *J Appl Physiol* 22: 333–337, 1967.